

Microwave dynamic large signal waveform characterization of advanced InGaP HBT for power amplifiers

Zhao Lixin(赵立新)[†], Jin Zhi(金智), and Liu Xinyu(刘新宇)

(Institute of Microelectronics, Chinese Academy of Sciences, Beijing 100029, China)

Abstract: In wireless mobile communications and wireless local area networks (WLAN), advanced InGaP HBT with power amplifiers are key components. In this paper, the microwave large signal dynamic waveform characteristics of an advanced InGaP HBT are investigated experimentally for 5.8 GHz power amplifier applications. The microwave large signal waveform distortions at various input power levels, especially at large signal level, are investigated and the reasons are analyzed. The output power saturation is also explained. These analyses will be useful for power amplifier designs.

Key words: large signal dynamic characteristics; InGaP HBT; waveform distortion

DOI: 10.1088/1674-4926/30/12/124008

EEACC: 7280E; 7360L

1. Introduction

Wireless communication systems and local area networks (WLAN) are spreading out worldwide. Wireless cities are being built around the world. WLAN compatible notebook computers and handheld devices are being used by more and more people. WLAN systems utilize an orthogonal frequency division multiplexing modulation scheme and operate in the 2.4 GHz and 5.8 GHz frequency bands. This is critical to microwave amplifiers and microwave transistors^[1]. Modern advanced microwave indium gallium phosphide heterojunction bipolar transistors (InGaP HBT) are key components used in microwave power amplifiers in wireless mobile communication and WLAN^[2, 3].

Microwave amplifiers and transistors in wireless communication and WLAN are usually used for linear power amplification. However, with increasing input power, the transistor and amplifier will not work linearly at high power levels. Investigation of the microwave dynamic large signal voltage and current waveforms in the time domain at high power levels will give a more precise device characteristic picture^[4-6]. With increasing input power, output power increases accordingly at a small signal level, but will not increase linearly at high power levels. Precisely observing and analyzing the microwave dynamic large signal voltage waveforms and current waveforms is of benefit to microwave power amplifier design^[7, 8].

In this paper, the microwave dynamic large signal voltage waveforms and current waveforms of a modern advanced InGaP/GaAs HBT cell are investigated experimentally for 5.8 GHz microwave amplifier design applications. The microwave dynamic large signal characteristics of the InGaP HBT are analyzed experimentally in the time and frequency domains. Firstly, the dynamic microwave voltage waveforms and cur-

rent waveforms are investigated at a small signal injection level, at the -1 dB gain compression point, at the -3 dB gain compression point, and at the maximum saturation output power point respectively. Then the microwave dynamic input voltage spectrum, input current spectrum, output voltage spectrum and current spectrum are analyzed, and the major factors that cause voltage waveform and current waveform distortion are also analyzed. Finally, we draw some conclusions on the reasons for microwave large signal waveform distortions at the -1 dB gain compression point, at the -3 dB gain compression point, and at the saturation output power point respectively.

2. Microwave dynamic large signal waveforms

In general the output power of a microwave transistor increases with increasing input power, and it is used to linearly

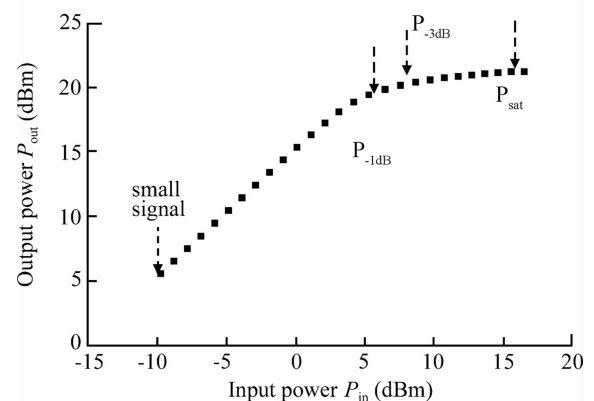


Fig. 1. Output power versus input power as measured. Microwave waveform measurement points are marked on the curve of output power versus input power from a small signal up to saturation output power. The device is biased at $V_{CE} = 3.61$ V, $I_C = 53.7$ mA, $V_{BE} = 1.28$ V.

[†] Corresponding author. Email: zhaolixin@ime.ac.cn

Received 23 June 2009, revised manuscript received 14 August 2009

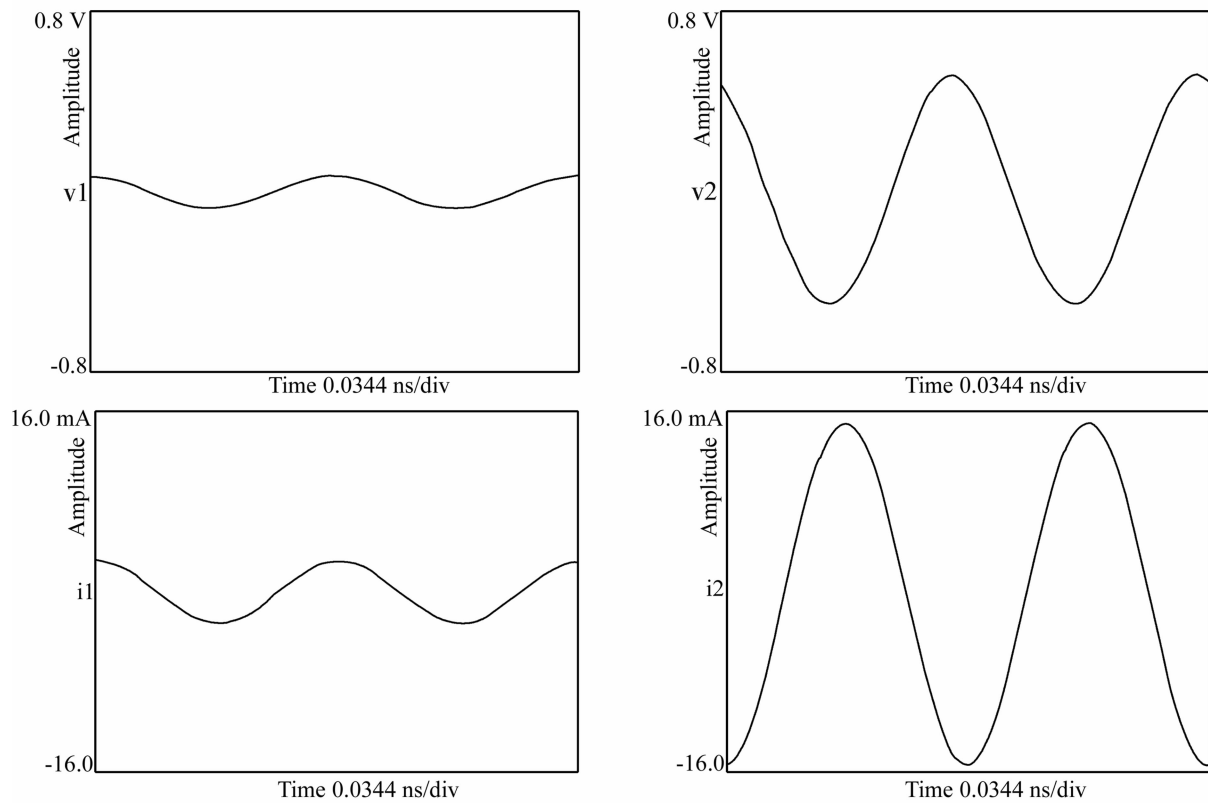


Fig. 2. Microwave current and voltage waveforms measured at input port (v_1 , i_1) and output port (v_2 , i_2) when injecting a microwave small signal at frequency $f_0 = 5.8$ GHz. The device is biased at $V_{CE} = 3.607$ V, $I_C = 53.7$ mA, $V_{BE} = 1.283$ V. Microwave small signal input power $P_{in} = -9.72$ dBm, microwave output power $P_{out} = 5.64$ dBm, transistor transducer gain $G_T = 15.36$ dB.

amplify the microwave signal. But the device is essentially nonlinear. In this investigation, the amplifier transistor is an InGaP/GaAs/GaAs npn transistor cell with a device area around 1×10^{-3} mm². The transistor DC current gain is $\beta = 80$, and the collector-emitter breakdown voltage is about 12 V. The transistor maximum oscillation frequency is around 110 GHz, and the unit current gain frequency is about 40 GHz.

The transistor cell is measured on-wafer using Pico-Probe ground-signal-ground (GSG) probes and a Cascade test station in an AgilentN5242 nonlinear vector network analyzer system^[9,10]. The power device is matched for maximum output power at $\Gamma_{source} = 0.4748 \angle 60.32$ deg, $\Gamma_{load} = 0.2503 \angle 46.48$ deg with a match system.

While injecting a sinusoidal signal and increasing the input power level, the voltage waveforms and current waveforms at the input and output ports are investigated at a small signal injection level, at the -1 dB gain compression point P_{-1dB} , at the -3 dB gain compression point P_{-3dB} , and at the maximum saturation output power point P_{sat} respectively, as shown in Fig. 1.

2.1. Microwave waveform at a small signal injection level

While injecting a microwave small signal at frequency $f = 5.8$ GHz, the microwave voltage waveforms and current waveforms of v_1 , i_1 at the input port, and v_2 , i_2 at the output port are measured as shown in Fig. 2. The microwave small signal input power is $P_{in} = -9.72$ dBm, the microwave output power is $P_{out} = 5.64$ dBm, and transistor transducer gain is

$G_T = 15.36$ dB. Both the microwave voltage waveforms and current waveforms are ideal sinusoidal waveforms at the input and output ports at a small signal level.

2.2. Microwave large signal waveform at the -1 dB gain compression point

As the input power increases from the small signal level, the output power increases accordingly. Figure 3 shows the microwave current and voltage waveforms at the -1 dB gain compression point, P_{-1dB} at frequency 5.8 GHz. At this point the input power is $P_{in} = 5.03$ dBm, the microwave output power is $P_{out} = 19.39$ dBm and the microwave power gain is $G_T = 14.36$ dB. At the -1 dB gain compression point, the output voltage waveform is not a critical sinusoidal waveform, but the output current waveform is similar to sinusoidal, as Figure 3 shows.

2.3. Microwave large signal waveform at the -3 dB gain compression point

When increasing the input microwave power level continually from P_{-1dB} point, the output power level increases accordingly but not linearly. Figure 4 shows the microwave current and voltage waveforms at the -3 dB gain compression point, P_{-3dB} . At this point, microwave signal input power is $P_{in} = 8.01$ dBm, output power is $P_{out} = 20.37$ dBm and power gain is $G_T = 12.36$ dB. The microwave power gain is about 3 dB lower than the small signal power gain. Obviously both the output voltage waveform and the input voltage waveform are distorted.

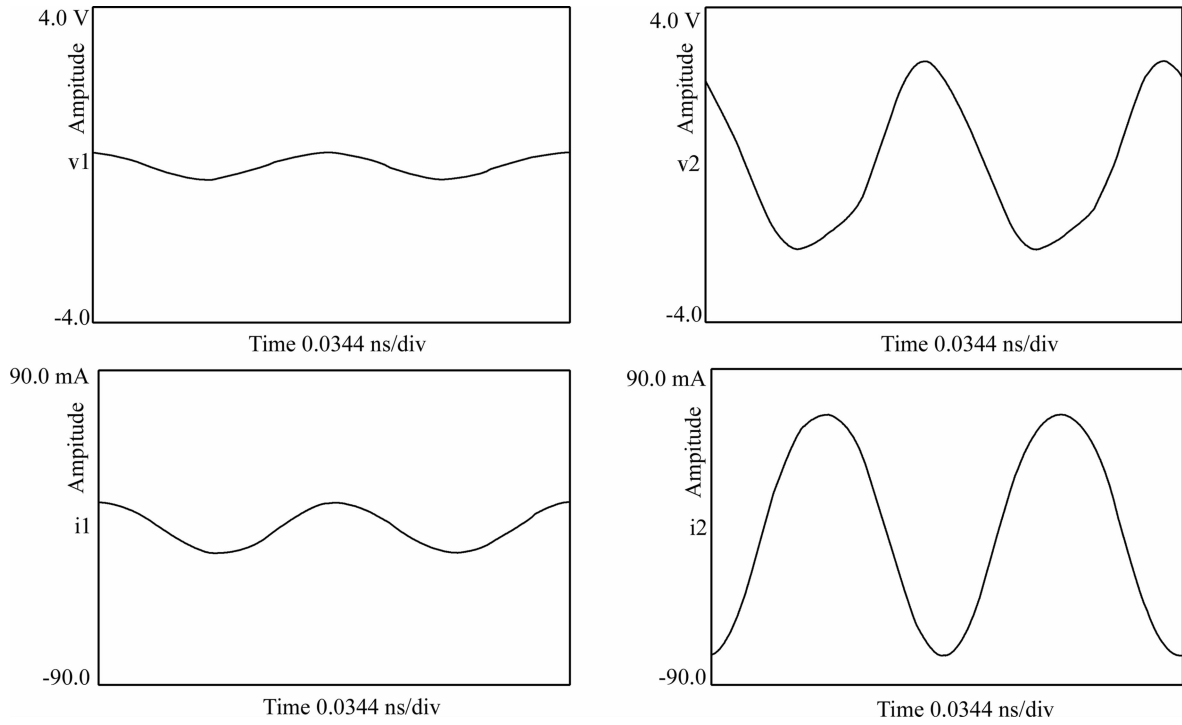


Fig. 3. Microwave large signal current and voltage waveforms measured at input port (v_1, i_1) and output port (v_2, i_2) at the -1 dB power gain compression point. The device is biased at $V_{CE} = 3.607$ V, $I_C = 53.7$ mA, $V_{BE} = 1.283$ V. Microwave input power $P_{in} = 5.03$ dBm, output power $P_{out} = 19.39$ dBm, power gain $G_T = 14.36$ dB.

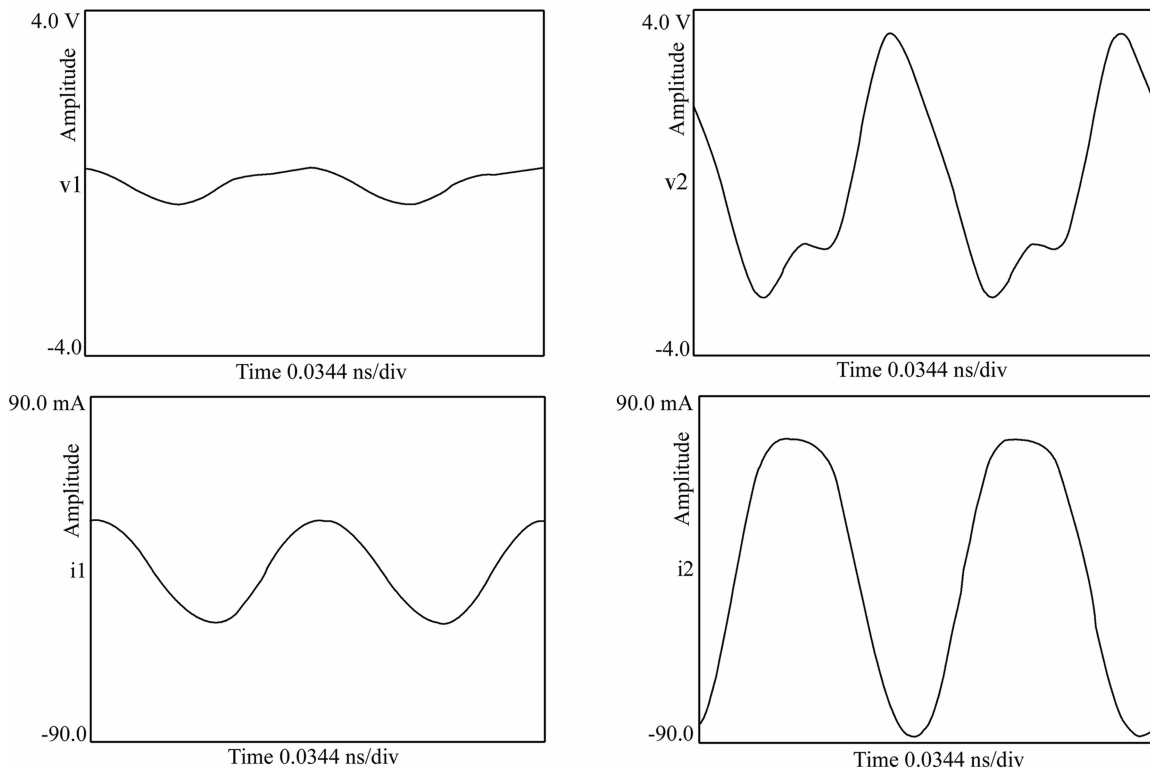


Fig. 4. Measured microwave current and voltage waveforms of v_1, i_1 at input port and v_2, i_2 at output port at the -3 dB compression point. The device is biased at $V_{CE} = 3.607$ V, $I_C = 53.7$ mA, $V_{BE} = 1.283$ V. The microwave input power $P_{in} = 8.01$ dBm, output power $P_{out} = 20.37$ dBm, power gain $G_T = 12.36$ dB.

2.4. Microwave large signal waveform at the saturation output power point

If the input power from the P_{-3dB} point keeps increasing, the output power will become saturated and reaches the

maximum output power. The microwave large signal current and voltage waveforms are shown in Fig. 5. When the device output power is saturated, the microwave input power is $P_{in} = 16.55$ dBm, the microwave saturation output power is $P_{sat} = 21.41$ dBm, and the power gain is $G_T = 4.86$ dB. Both the

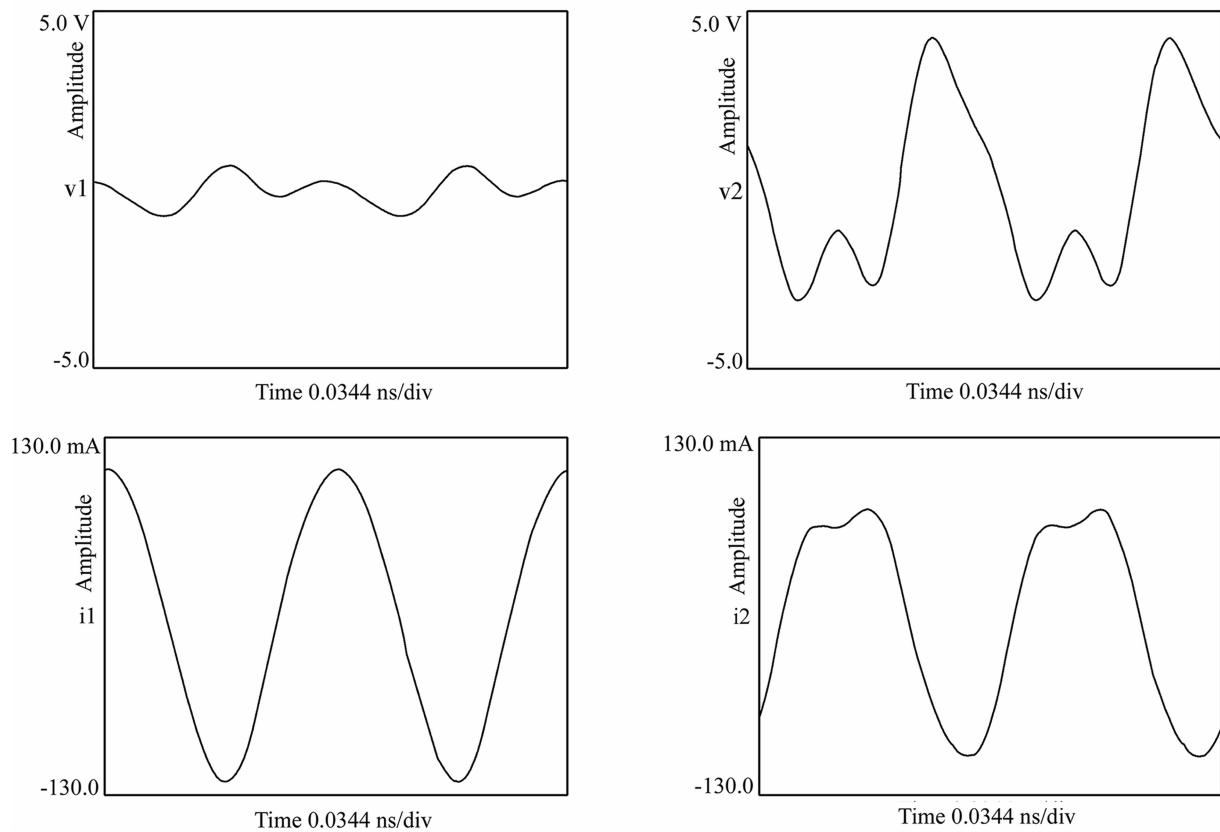


Fig. 5. Measured microwave large signal current and voltage waveforms of v_1 , i_1 at input port and v_2 , i_2 at output port when the device output power is saturated. The device is biased at $V_{CE} = 3.607$ V, $I_C = 53.7$ mA, $V_{BE} = 1.283$ V. The device microwave input power $P_{in} = 16.55$ dBm, microwave saturation output power $P_{sat} = 21.41$ dBm, power gain $G_T = 4.86$ dB.

output voltage waveform and the input voltage waveform are seriously distorted under saturation output power conditions. The output current waveform is also seriously distorted.

3. Discussion

For convenience of discussion in the following subsections, all of the voltage values and current values with multi-frequency components at the input and output ports are listed in Table 1.

3.1. At the small signal level

The microwave small signal current spectra and voltage spectra are shown in Fig. 6 and in Table 1. The microwave voltage is amplified about 17 dB, and microwave current is amplified around 14.8 dB. At the small signal injection level, there is no second harmonic voltage or third harmonic voltage observed at the output or input ports. Additionally, there is no visible second harmonic current or third harmonic current at the output and input ports. It can be seen that the microwave voltage and current are amplified almost without distortion at the small signal level.

3.2. At the P_{-1dB} point

With input power continually increasing from the small signal, the power gain will decrease. The microwave large signal current spectra and voltage spectra at the -1 dB gain compression point are shown in Fig. 7 and Table 1. At this point,

the microwave fundamental voltage is amplified about 16.8 dB, and the microwave fundamental current is amplified about 13.8 dB. It can be seen that with input power increasing from the small signal level, the second and third harmonic components of voltage and current begin to appear at the output port and increase further. Obviously the output second harmonic voltage (12.3% of the fundamental output voltage) is a major factor of the output voltage waveform distortion.

3.3. At the microwave large signal P_{-3dB} point

With input power continually increasing from the P_{-1dB} point, the second harmonic components and third harmonic components of voltage and current appear significantly at the input port. The microwave current and voltage frequency spectrum diagrams measured at the input port (v_1 , i_1) and at the output port (v_2 , i_2) at the -3 dB gain compression point are shown in Fig. 8 and Table 1. The fundamental voltage is amplified about 16.8 dB and the fundamental current is amplified about 9.6 dB. Compared with the situation of the P_{-1dB} point, not only the output second harmonic voltage (about 25% of the output fundamental voltage) but also the input second harmonic voltage (about 22% of the input fundamental voltage) are major factors in the voltage wave distortion. So, both the input second harmonic voltage and the output second harmonic voltage are major factors in microwave signal distortion. In addition, at the large signal injection level of the P_{-3dB} point, the input port voltage has distorted already, cons-

Table 1. Current and voltage values at input and output ports.

Input port	Small signal (V, mA)	P_{-1dB} point (V, mA)	P_{-3dB} point (V, mA)	Sat. power point (V, mA)
Voltage at fundamental freq.	0.072 V \angle 2.685 deg	0.338 V \angle 9.529 deg	0.394 V \angle 24.179 deg	0.352 V \angle 101.906 deg
Voltage at 2 nd harmonic freq.	0	0	0.087 V \angle -87.940 deg 22% of the input fundamental voltage	0.428 V \angle -30.023 120% of the fundamental input voltage
Voltage at 3 rd harmonic freq.	0	0	0.031 V \angle 18.999 deg 7.9% of the input fundamental voltage	0.087 V \angle 108.020 deg 24.7% of the input fundamental voltage
Current at fundamental freq.	2.760 mA \angle -1.398 deg	14.444 mA \angle -4.447 deg	27.267 mA \angle -9.345 deg	113.119 mA \angle -3.495 deg
Current at 2 nd harmonic freq.	0	0	1.363 mA \angle 96.096 deg 5% of the input fundamental current	6.701 mA \angle 154.016 deg 5.9% of the fundamental input current
Current at 3 rd harmonic freq.	0	0	0.674 mA \angle -175.695 deg 2.5% of the input fundamental current	1.881 mA \angle -86.107 deg 1.7% of the fundamental input current
Output port	Small signal (V, mA)	P_{-1dB} point (V, mA)	P_{-3dB} point (V, mA)	Sat. power point (V, mA)
Voltage at fundamental freq.	0.506 V \angle 19.808 deg	2.349 V \angle 25.188 deg	2.731 V \angle 42.964 deg	3.081 V \angle 61.242 deg
Voltage at 2 nd harmonic freq.	0	0.289 V \angle 46.097 deg 12.3% of the fundamental output voltage	0.684 V \angle 69.991 deg 25% of the output fundamental voltage	1.134 V \angle 122.239 deg 36.8% of the fundamental output voltage
Voltage at 3 rd harmonic freq.	0	0.145 V \angle 168.146 deg	0.438 V \angle -145.054 deg 16% of the output fundamental voltage	0.907 V \angle -61.403 deg 29.4% of the output fundamental voltage
Current at fundamental freq.	15.190 mA \angle -177.679 deg	70.534 mA \angle -172.331 deg	82.020 mA \angle -154.555 deg	92.534 mA \angle -136.275 deg
Current at 2 nd harmonic freq.	0	4.119 mA \angle -167.247 deg 5.8% of the fundamental output current	9.745 mA \angle -143.346 deg 11.9% of the output fundamental current	15.152 mA \angle -91.094 deg 16.4% of the fundamental output current
Current at 3 rd harmonic freq.	0	1.596 mA \angle 36.663 deg	4.821 mA \angle 83.460 deg 5.9% of the output fundamental current	9.986 mA \angle 167.109 deg 10.8% of the fundamental output current

equently causing more serious distortion at the output port.

3.4. At the microwave large signal P_{sat} point

As the input power from the P_{-3dB} point is increasing, the output power will be saturated soon. The current and voltage spectra at the output port (v_2, i_2) and at the input port (v_1, i_1) are shown in Fig. 9 and in Table 1. The fundamental voltage is amplified about 18.8 dB; the fundamental current is amplified about -1.74 dB.

It can be seen that not only the input second harmonic voltage and output second harmonic voltage but also the input third harmonic voltage and the output third harmonic voltage are major factors of signal waveform distortion. These harmonic components occupy more than 1/4 of their individual fundamental components.

At the input port the second harmonic voltage has become greater than the fundamental voltage. This is a nonideal voltage; it worsens the input voltage waveform quality and

worsens the output voltage waveform quality further. A possible reason for the input port second harmonic voltage becoming greater than the fundamental voltage is that the reflected voltage becomes significant at the input port at very large power level. The reflected voltage superposes on the forward voltage and causes the second harmonic voltage to be greater than the fundamental voltage.

The fundamental current is not amplified but is scaled down compared with the input fundamental current; this will reduce the increasing fundamental output power trend. If output current I_{out} decreases, the output power $P_{out} = I_{out}V_{out}$ will not increase. Some possible reasons for fundamental current non-amplification are analyzed as follows. Under large power injection conditions, the forward voltage may become large, the hole injection barrier is reduced, and many excess holes inject into the emitter. This decreases the injection efficiency, causing the current gain to decrease^[11]. Secondly, at the saturation power point, the observed output fundamental current

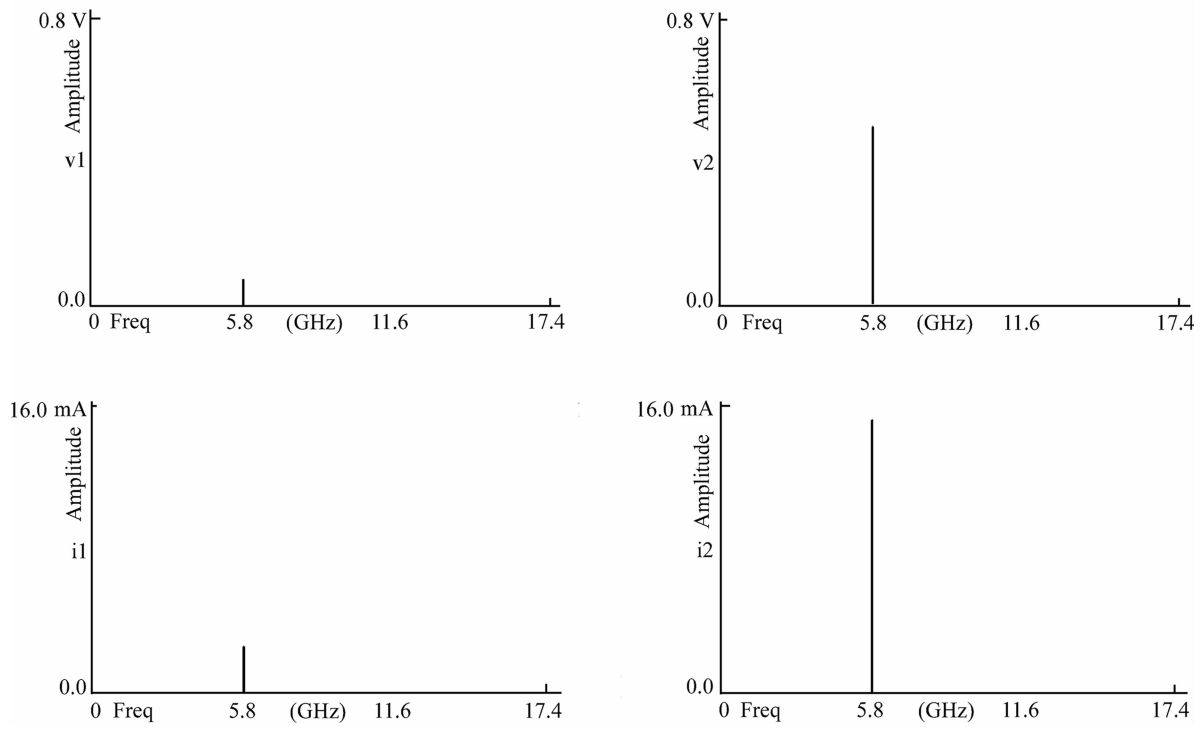


Fig. 6. Microwave current and voltage frequency spectra measured at input port (v_1, i_1) and at output port (v_2, i_2) when injecting a small signal at frequency $f_0 = 5.8$ GHz. The device is biased at $V_{CE} = 3.607$ V, $I_C = 53.7$ mA, $V_{BE} = 1.283$ V. Microwave input power $P_{in} = -9.72$ dBm, microwave output power $P_{out} = 5.64$ dBm, transducer gain $G_T = 15.36$ dB.

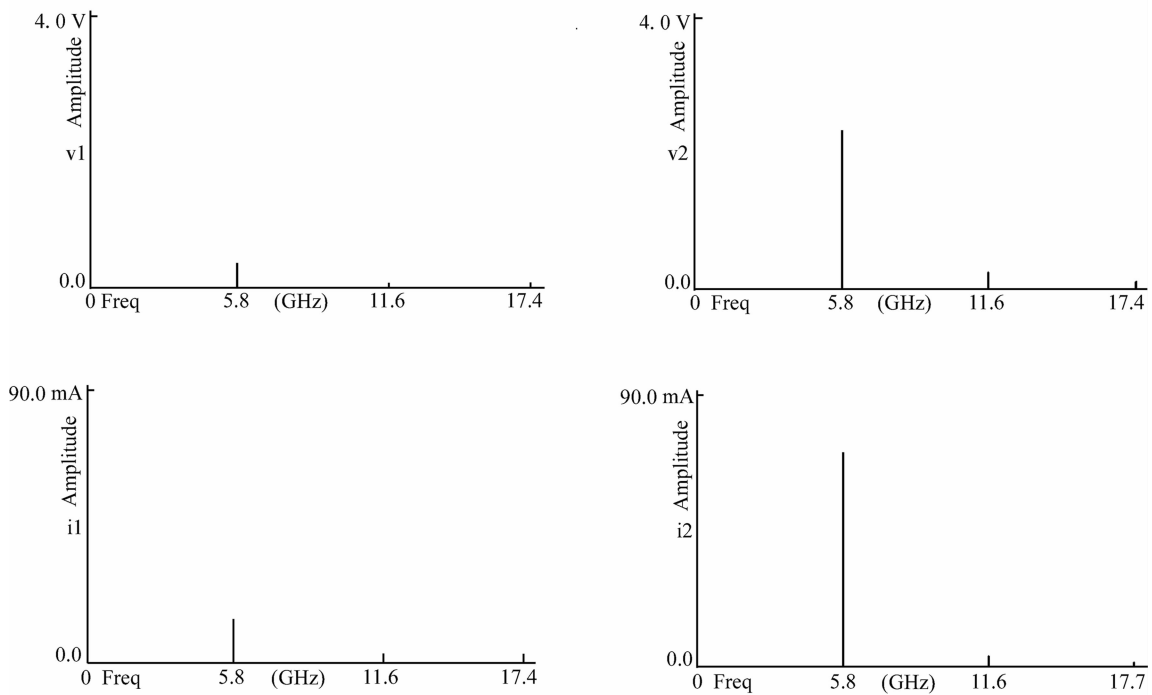


Fig. 7. Microwave current and voltage frequency spectra at input port (v_1, i_1) and at output port (v_2, i_2) measured at the -1 dB gain compression point. The device is biased at $V_{CE} = 3.607$ V, $I_C = 53.7$ mA, $V_{BE} = 1.283$ V. The microwave input power $P_{in} = 5.03$ dBm, output power $P_{out} = 19.39$ dBm, gain $G_T = 14.36$ dB. The power gain is compressed about by 1 dB compared to the small signal one.

is $I_2(f_0) = 92.534$ mA, the observed input fundamental current is $I_1(f_0) = 113.119$ mA, and the transistor DC bias collector current is $I_C = 53.7$ mA. It can be seen that the output current amplitude is much greater than the DC bias current. Under these conditions, the output current exceeds the transistor

operation area, and gets into the transistor cut off area or saturation area; the output current maintains the value within the transistor operation area, and it cannot be amplified further. Thirdly, at the saturation power point the harmonic currents take more current percentages than at the P_{-3dB} point or at

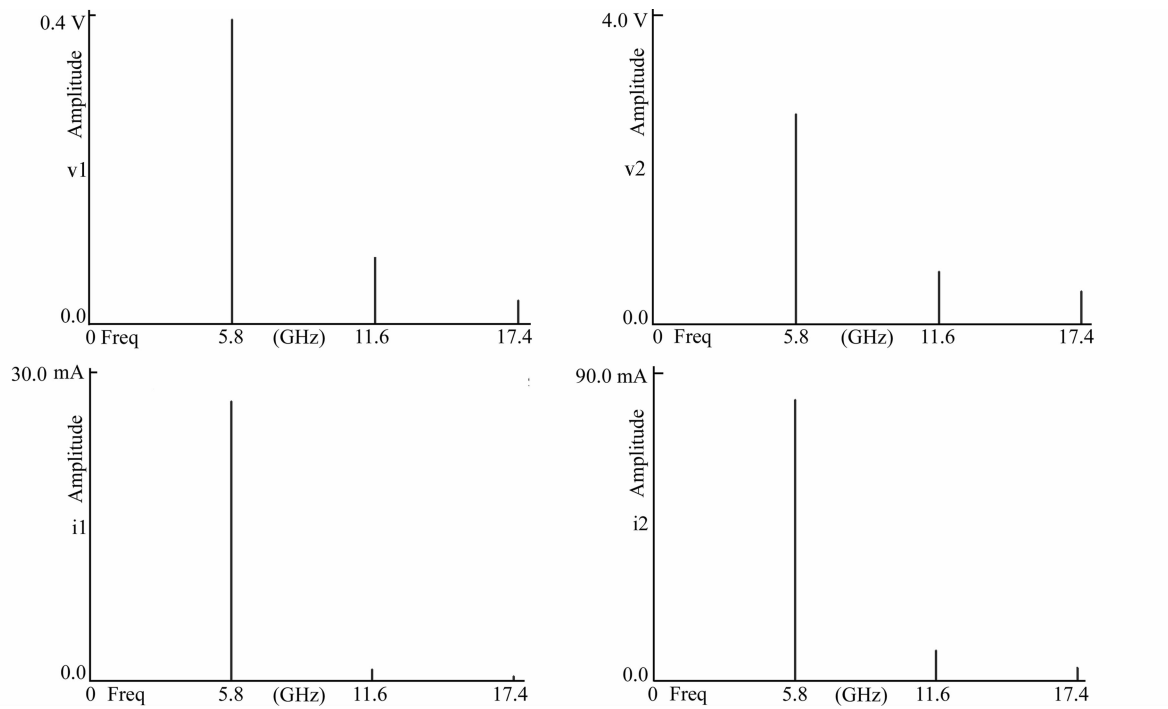


Fig. 8. Microwave current and voltage frequency spectra measured at input port (v_1, i_1) and at output port (v_2, i_2) at -3 dB gain compression point. The device is biased at $V_{CE} = 3.607$ V, $I_C = 53.7$ mA, $V_{BE} = 1.283$ V. The input power $P_{in} = 8.01$ dBm, output power $P_{out} = 20.3$ dBm, transducer gain $G_T = 12.36$ dB.

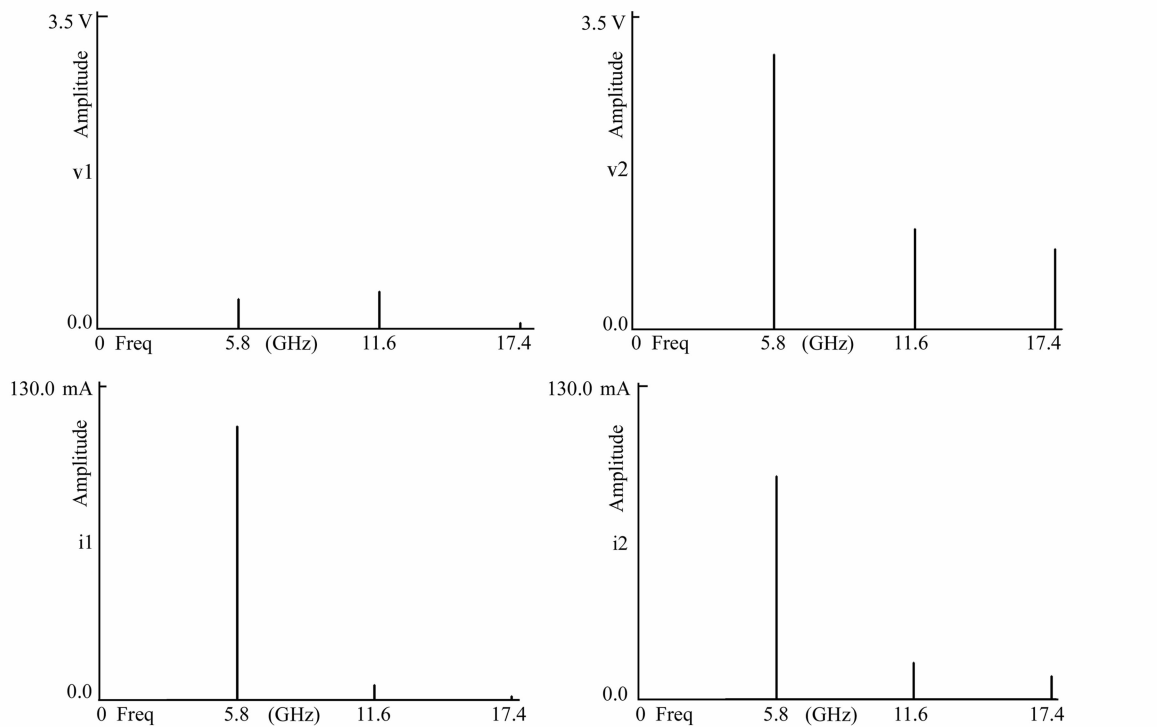


Fig. 9. Microwave current and voltage frequency spectra of input port (v_1, i_1) and output port (v_2, i_2) at saturated output power point. The device is biased at $V_{CE} = 3.607$ V, $I_C = 53.7$ mA, $V_{BE} = 1.283$ V. The device microwave input power $P_{in} = 16.55$ dBm, microwave saturation output power $P_{sat} = 21.41$ dBm, power gain $G_T = 4.86$ dB.

lower power level points. The second harmonic output current (16%) and third harmonic output current (11%) occupy more percentages of the fundamental output current at the saturation power point compared with the second harmonic output current occupation (12%) and third harmonic output current occupation (6%) at the P_{-3dB} point.

4. Conclusion

In this paper, the microwave dynamic large signal waveform characteristics of a modern advanced InGaP HBT are investigated experimentally at a small signal level, at the -1 dB gain compression point, at the -3 dB gain compression

point, and at the maximum saturation output power point respectively.

At the small signal level, the microwave signal is amplified linearly. With input power increasing from the small signal, the output power increases correspondingly; meanwhile, distortions appear. At the -1 dB gain compression $P_{-1\text{dB}}$ point, the output second harmonic voltage is the major factor of microwave waveform distortion. At the -3 dB gain compression $P_{-3\text{dB}}$ point, not only the output second harmonic voltage but also the input second harmonic voltage are the major factors of microwave signal distortion. At the saturation output power P_{sat} point, besides the input and output second harmonic voltages, the input and output third harmonic voltages are the major factors of microwave signal distortion. Meanwhile, at power saturation, the input second harmonic voltage becomes greater than the fundamental input voltage. This nonideal voltage worsens the waveform quality.

At a very large input power level the output power reaches saturation. A possible reason observed for this is that the fundamental input current is not amplified but scaled down. The output power will not increase with increasing input power at the saturation output power point.

References

- [1] Cripps S. Microwave power amplifiers for wireless communications. New York: Artech House, 2006
- [2] Hattori R. Manufacturing technology of InGaP HBT power amplifiers for cellular phone applications. GaAs Mantech Digest, April 2002: 241
- [3] Aditya G, InGaP HBT vs CMOS for mobile handset power amps. EETimes, June 2007
- [4] Groote V, Jardel O, Verspecht J, et al. Time domain harmonic load-pull of an AlGaIn/GaN HEMT. The 66th ARFTG Conference Washington, District of Columbia, USA, December 2005
- [5] Hecham S, Nkbus J M, QuBrk R, et al. Measurement and modeling of static and dynamic breakdowns of power GaInP/GaAs HBTs. IEEE MTT-S Digest, August 2002
- [6] Clark C J, Chrisikos G, Muha M S, et al. Time-domain envelope measurement technique with application to wideband power amplifier modeling. IEEE Trans Microw Theory Technol, 1998, 46(12): 2531
- [7] Verbeyst F, Bossche M V. Real-time and optimal PA characterization speeds up PA design. 34th European Microwave Conference Digest, Oct 2004, 10: 431
- [8] Reveyrand T, Maziere C, Nebus J M, et al. A calibrated time domain envelope measurement system for the behavioral modeling of power amplifiers. Eur Microw Week GaAs, Milan, Italy, Sep 2002, 9: 237
- [9] Agilent, Large signal network analyzer brochure, 2009
- [10] Blockley P, Gunyan V, Scott J. Mixer-based vector-corrected vector Signal/network analyzer offering 300 kHz – 20 GHz bandwidth and traceable phase response. IEEE International Microwave Symposium Digest, June 2005, 6: 1497
- [11] Anderson B L, Anderson R L. Fundamental of semiconductor devices. New York: McGraw Hill Companies Inc, 2005